Biochimica et Biophysica Acta 1847 (2015) 526–533

Contents lists available at ScienceDirect

Biochimica et Biophysica Acta

journal homepage: www.elsevier.com/locate/bbabio

Skeletal muscle mitochondria of *NDUFS4*$^{-/-}$ mice display normal maximal pyruvate oxidation and ATP production

Mohammad T. Alam [a,b,1,2], Ganesh R. Manjeri [a,b,2], Richard J. Rodenburg [b,c], Jan A.M. Smeitink [b,c], Richard A. Notebaart [b,d], Martijn Huynen [b,d], Peter H.G.M. Willems [a,b], Werner J.H. Koopman [a,b,*]

[a] Department of Biochemistry, RIMLS, Radboud University Medical Center, Nijmegen, The Netherlands
[b] Centre for Systems Biology and Bioenergetics, Radboud University Medical Centre, Nijmegen, The Netherlands
[c] Department of Pediatrics, NCMD, Radboud University Medical Center, Nijmegen, The Netherlands
[d] Centre for Molecular and Biomolecular Informatics, RIMLS, Radboud University Medical Center, Nijmegen, The Netherlands

ARTICLE INFO

Article history:
Received 13 August 2014
Received in revised form 3 February 2015
Accepted 7 February 2015
Available online 14 February 2015

Keywords:
CI, complex I
IMS, inter-membrane space
MIM, mitochondrial inner membrane
MOM, mitochondrial outer membrane
ODE, ordinary differential equation
ETC, electron transport chain

ABSTRACT

Mitochondrial ATP production is mediated by the oxidative phosphorylation (OXPHOS) system, which consists of four multi-subunit complexes (CI–CIV) and the F_oF_1-ATP synthase (CV). Mitochondrial disorders including Leigh Syndrome often involve CI dysfunction, the pathophysiological consequences of which still remain incompletely understood. Here we combined experimental and computational strategies to gain mechanistic insight into the energy metabolism of isolated skeletal muscle mitochondria from 5-week-old wild-type (WT) and CI-deficient *NDUFS4*$^{-/-}$ (KO) mice. Enzyme activity measurements in KO mitochondria revealed a reduction of 79% in maximal CI activity (V_{max}), which was paralleled by 45–72% increase in V_{max} of CII, CIII, CIV and citrate synthase. Mathematical modeling of mitochondrial metabolism predicted that these V_{max} changes do not affect the maximal rates of pyruvate (PYR) oxidation and ATP production in KO mitochondria. This prediction was empirically confirmed by flux measurements. *In silico* analysis further predicted that CI deficiency altered the concentration of intermediate metabolites, modestly increased mitochondrial NADH/NAD^+ ratio and stimulated the lower half of the TCA cycle, including CII. Several of the predicted changes were previously observed in experimental models of CI-deficiency. Interestingly, model predictions further suggested that CI deficiency only has major metabolic consequences when its activity decreases below 90% of normal levels, compatible with a biochemical threshold effect. Taken together, our results suggest that mouse skeletal muscle mitochondria possess a substantial CI overcapacity, which minimizes the effects of CI dysfunction on mitochondrial metabolism in this otherwise early fatal mouse model.

1. Introduction

Mitochondria are among the prime producers of cellular ATP and consist of a matrix compartment surrounded by an inner (MIM) and outer membrane (MOM), with in between an inter-membrane space (IMS) [1–9]. Mitochondrial ATP production is fueled by pyruvate (PYR), two molecules of which are generated from glucose (GLU) by glycolysis in the cytosol. PYR can be reversibly converted by lactate dehydrogenase (LDH) into lactate or imported into the mitochondrial matrix by a dedicated pyruvate carrier [10]. Within the mitochondrion PYR is converted into acetyl coenzyme A (acetyl-CoA) that enters the tricarboxylic acid (TCA) cycle to yield two molecules of CO_2, one molecule of ATP, four molecules of NADH and one molecule of $FADH_2$. NADH and $FADH_2$ serve as substrates for the oxidative phosphorylation (OXPHOS) system to generate ATP [2,5]. The OXPHOS system consists of four multi-subunit complexes (CI–CIV) that form the electron transport chain (ETC) and the ATP-generating F_oF_1-ATPase (CV). Within the ETC. electrons donated by NADH (at CI) and $FADH_2$ (at CII) are transported to CIII and CIV by coenzyme Q_{10} (CoQ_{10}) and cytochrome-*c* (cyt-*c*), respectively. At CIV, electrons are donated to molecular oxygen (O_2) to form water. The energy released during electron transport is utilized at CI, CIII and CIV to transport H^+ out of the mitochondrial matrix across the MIM. This process generates an inward-directed proton-motive

Abbreviations: Δψ, mitochondrial membrane potential; CI, complex I; ETC, electron transport chain; KO, knockout; IMS, inter-membrane space; MIM, mitochondrial inner membrane; MOM, mitochondrial outer membrane; ODE, ordinary differential equation; OXPHOS, oxidative phosphorylation; WT, wild-type

* Corresponding author at: 286 Biochemistry, Radboud Institute for Molecular Life Sciences (RIMLS), Radboud University Medical Center (RUMC), P.O. Box 9101, NL-6500 HB Nijmegen, The Netherlands. Tel.: +31 24 3614589; fax: +31 24 3616413.
E-mail addresses: mta26@cam.ac.uk (M.T. Alam), Ganesh.Manjeri@radboudumc.nl (G.R. Manjeri), Richard.Rodenburg@radboudumc.nl (R.J. Rodenburg), Jan.Smeitink@radboudumc.nl (J.A.M. Smeitink), Richard.Notebaart@radboudumc.nl (R.A. Notebaart), Martijn.Huijnen@radboudumc.nl (M. Huynen), Peter.Willems@radboudumc.nl (P.H.G.M. Willems), Werner.Koopman@radboudumc.nl (W.J.H. Koopman).
[1] Current address: Dept. of Biochemistry, 80 Tennis Court Road, Sanger Building, CB2 1GA, Cambridge, United Kingdom.
[2] First authorship contribution: These authors equally contributed to the study.

http://dx.doi.org/10.1016/j.bbabio.2015.02.006
0005-2728/

force (PMF) consisting of an electrical ($\Delta\Psi$) and chemical component (ΔpH). At CV the energy associated with H^+ re-entry into the mitochondria matrix is used to generate ATP from ADP and inorganic phosphate (P_i).

In addition to ATP generation, mitochondria play a key role in various other cellular processes, including reactive oxygen species (ROS) generation, calcium signaling and apoptosis induction. Therefore it is not surprising that dysfunction of the OXPHOS system, which sustains most mitochondrial functions, is associated with a broad range of human disorders [11–17]. Among OXPHOS disorders, deficiency of CI (OMIM 252010) is the most common [18–26]. Human CI deficiency is associated with a wide range of clinical presentations including muscle weakness, heart disease, liver failure, respiratory failure and congenital lactic acidosis, often leading to death in early childhood [11,21,24–27]. CI is the largest protein complex of the oxidative phosphorylation system and consists of 44 different proteinaceous subunits that are encoded by either the mitochondrial (mtDNA) or nuclear DNA [28–30]. Regarding the cellular consequences of nDNA-encoded CI mutations, several studies with primary patient fibroblast have been carried out revealing aberrations in maximal ETC. enzyme activities (V_{max}) and mitochondrial morphology, increased levels of cellular reactive oxygen species (ROS) and disturbed calcium and ATP homeostasis [28,31–36].

Recently a whole-body KO mouse model of human CI deficiency became available in which one of the CI accessory subunit genes (*NDUFS4*) is deleted [24]. The *NDUFS4* gene encodes an 18-kDa protein (NDUFS4 or NADH dehydrogenase (ubiquinone) Fe-S protein 4). When NDUFS4 is absent, proper CI assembly is hampered and its V_{max} is reduced [20,21,23,24,26,37,38]. Importantly, several symptoms of human CI deficiency are also observed in *NDUFS4*$^{-/-}$ animals such as developmental delays, failure to thrive, lethargy, opthalmoplegia and progressive encephalomyopathy leading to early lethality. However, the consequences of *NDUFS4* gene deletion on mitochondrial energy metabolism, its underlying reaction rates and reactant concentrations have not been investigated yet. Here we addressed this question by combining experimental and computational strategies to evaluate: (i) if *NDUFS4* knockout affected the V_{max} of key ETC enzymes and citrate synthase (CS), and (ii) whether *NDUFS4* knockout impacted on the maximal rates of PYR oxidation and ATP production in isolated skeletal muscle mitochondria. To this end we first adapted a previously validated dynamic model of mitochondrial metabolism [39] to our experimental conditions. Next, we used this model to predict the consequences of *NDUFS4* knockout on the steady-state values of metabolic fluxes, metabolite concentrations and physiological variables including $\Delta\psi$. This analysis predicted that a reduction of ~80% in the V_{max} of CI did not affect the maximal rates of mitochondrial PYR oxidation and ATP production in isolated *NDUFS4*$^{-/-}$ skeletal muscle mitochondria. This prediction was confirmed by experimental flux analysis and suggests that these mitochondria possess a substantial CI overcapacity that limits the impact of CI deficiency on mitochondrial metabolism.

2. Materials and methods

2.1. Animals

NDUFS4$^{-/-}$ knockout (KO) and wild-type (WT) mice (mixed 129/Sv: C57BL6 background) were generated by crossing heterozygote (*NDUFS4*$^{+/-}$) mice. The genotype was confirmed by polymerase chain reaction (PCR) testing. Mice had *ad libitum* access to food and water and were fed on a standard animal diet (Ssniff GmbH, Soest, Germany: V1534-300 R/M-H). Animals were group housed at 22 °C and maintained on a day and night rhythm of 12 h. The animal studies were approved by the Regional Animal Ethics Committee (Nijmegen, The Netherlands) and performed under the guidelines of the Dutch Council for Animal Care. Both male and female animals were used in this study yielding similar results.

2.2. Measurement of maximal pyruvate oxidation, ATP production and enzymatic activities in mitoplasts

Skeletal muscle tissue from the entire hind limb was harvested from 5-week-old WT and KO animals, homogenized and centrifuged at 600 *g*. Importantly, maximal PYR oxidation rates, ATP production rates and enzymatic activities (V_{max}) were determined using the same 600 *g* supernatant using standardized protocols [40,41]. To quantify pyruvate oxidation, mitochondrial preparations were incubated with radiolabeled substrate ([1-^{14}C] pyruvate). After 20 min the reaction was stopped and the amount of liberated radioactive CO_2 ($^{14}CO_2$) was quantified [40]. The assay medium (pH 7.4) contained K^+-phosphate buffer (30 mM; source of P_i), KCl (75 mM), Tris (8 mM), K-EDTA (1.6 mM), P1,P5-Di (adenosine-5′) pentaphosphate (Ap5A; 0.2 mM), $MgCl_2$ (0.5 mM), ADP (2 mM), creatine (20 mM), malate (1 mM) and [1-^{14}C] pyruvate (1 mM). AP5A is a potent adenylate kinase (AK) inhibitor required to prevent interference of the AK reaction with the levels of produced ATP, as well as with the excess of ADP required for this assay. For ATP production measurements, the same assay medium was used but with pyruvate instead of [1-^{14}C] pyruvate. After 20 min, the reaction was stopped by addition of 0.1 M $HClO_4$. The reaction mixture was centrifuged at 14,000 *g* for 2 min at 2 °C. To the supernatant, 1.2 vol (V/V) of 0.333 M $KHCO_3$ was added, and this mixture was diluted 2-fold. The amount of ATP and phosphocreatine formed during the reaction was measured in the supernatant using a Konelab 20XT auto-analyzer (Thermo Scientific). Mitochondrial ATP production rate was corrected using a parallel assay in which residual glycolysis was blocked by arsenite (2 mM) [40]. The maximal activities of complex I (CI), complex II (CII), complex III (CIII), complex IV (CIV) and citrate synthase (CS) were measured in freeze-thawed 600 g supernatants, as described in [41].

2.3. Mathematical modeling and statistical analysis

Dynamic modeling and statistical analysis were performed using custom scripts written in Matlab 6.1 (Mathworks, Natick, Massachusetts, U.S.A.). The latter are available upon request. Unless stated otherwise, experimental data is presented as mean ± SEM (standard error of the mean) and statistical significance between datasets is assessed using an independent 2-population Student's *t*-test.

3. Results & discussion

3.1. Overall experimental and computational strategy

In this study we used mitochondria from skeletal muscle of wildtype (WT) mice and *NDUFS4*$^{-/-}$ (KO) mice for experimental analysis. Mitochondria were placed in an assay medium and were considered as a classical input–output (I/O) system (cartoon in Fig. 1), which converts pyruvate (PYR; input) into ATP (output) *via* the integrated action of transporters, the TCA cycle and the OXPHOS system (Fig. 2). To perform computational analysis of this system we adapted a mathematical model of the mitochondrial bioenergetic system that was previously validated by Beard and co-workers [39]. This model consists of a collection of ordinary differential equations (ODEs) and parameters, which allows integrated simulation of the above I/O system and prediction of the underlying fluxes, metabolite concentrations and physicochemical parameters. Our overall strategy (Fig. 1) aimed to first adapt the published model to the conditions under which PYR oxidation and ATP production are measured in our experimental assay medium (explained in more detail below). This yielded a mathematical model for isolated WT mitochondria ("WT model"). Next, the WT model was adjusted by including information regarding the measured maximum activities (V_{max}) of CI, CII, CIII, CIV and citrate synthase (CS) in mitochondria from WT and KO mice. This was achieved by multiplying the V_{max} values in the WT model by a "pre-factor" (KO/WT) corresponding to the experimentally observed change in

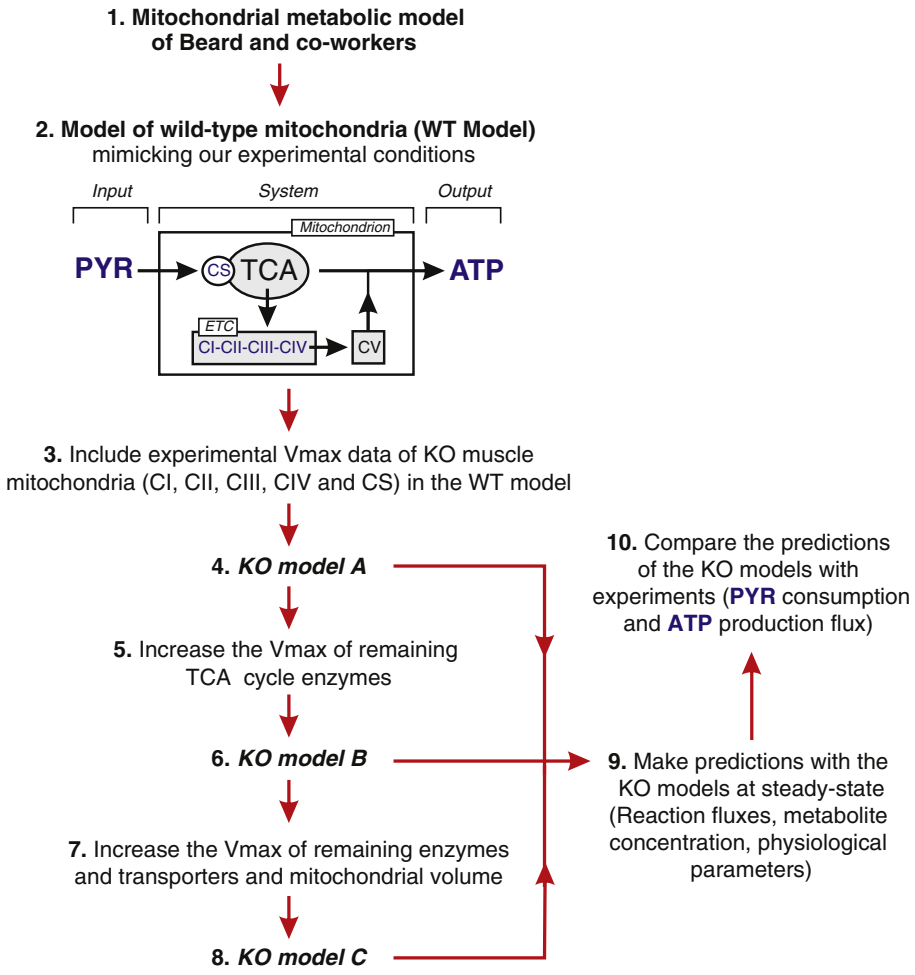

Fig. 1. Overall experimental and computational strategy. A mathematical model of mitochondrial metabolism developed by Beard and coworkers [39] was adapted to match our experimental conditions. This yielded a model for isolated mitochondria from skeletal muscle of wild-type mice (WT model). By including experimental data, the WT model was adapted to create various KO models (A, B and C) for simulating mitochondrial metabolism in isolated muscle mitochondria from *NDUFS4*$^{-/-}$ (KO) mice with isolated complex I deficiency. Predicted PYR oxidation and ATP consumption rates were compared with experimental flux measurements for model validation and predictive analysis (see main text for details).

these values for KO mitochondria. In this way a pre-factor >1 represented an increase in V_{max} for the KO *vs.* the WT condition, whereas a pre-factor <1 represented a decrease in V_{max} for the KO *vs.* the WT condition. We also generated two alternative KO models (KO model B and C) to simulate the consequences of increased CS activity with respect to TCA cycle enzyme activity and mitochondrial volume (see below for details). The KO models were used to predict the maximal PYR oxidation and ATP production rates (expressed as KO/WT ratios), which were compared with experimentally determined values for model validation, as well as other relevant reaction fluxes, metabolite concentrations and physiological parameters.

3.2. WT model

The model of Beard et al. [39] consists of three compartments (mitochondrial matrix, inter-membrane space and buffer space) and incorporates 43 flux expressions including TCA cycle fluxes, OXPHOS fluxes, substrate and cation fluxes, passive permeation fluxes and buffer reaction fluxes (Fig. 2). This model also contains various TCA control pathways including regulation of pyruvate dehydrogenase (PDH), α-ketoglutarate dehydrogenase (α-KGDH), aconitase (ACO) and fumarase (FUM; for a full list see Table 2 in [39]). All reactions in the model are thermodynamically balanced, and its parameters are validated using experimental data [39,42–46]. To generate the WT model we first removed metabolites, reactions and constant state variables from the Beard model that were not relevant under our experimental conditions (see Supplement for full details). These include two ATP-consuming reactions in the buffer space (*i.e.*, hexokinase and adenylate kinase), one reaction for passive AMP permeation, one adenylate kinase reaction in the inter-membrane space, and two substrate transport reactions (isocitrate and fumarate transport). Next, various metabolite concentrations were adapted to match the conditions of our experimental assay (*e.g.*, [PYR] = 1 mM, [P_i] = 30 mM, [malate] ([MAL]) = 1 mM, [ATP] = 0 mM, [ADP] = 2 mM; a full list is provided in Supplementary Table S2). The final WT model consisted of 46 state variables (including $\Delta\psi$) and 37 flux expressions. Analysis of this model at steady-state (*i.e.*, compatible with the experimental conditions of the PYR and ATP flux assays) yielded predictions of various fluxes, reactant concentrations and derived variables for the WT situation (Fig. 2A).

3.3. Experimental analysis of ETC. complex and citrate synthase in isolated skeletal muscle mitochondria from KO mice

The V_{max} of CI was reduced by 79% in KO *vs.* WT mitochondria (Table 1; "Experimental data, V_{max} values"). This reduction in CI activity was paralleled by a 45–72% increase in V_{max} of the other ETC. enzymes and of the TCA-cycle enzyme citrate synthase (CS).

3.4. KO models

To create KO model A, the V_{max} values for CI, CII, CIII, CIV and CS in the WT model were multiplied by the fractional change in this parameter in KO *vs.* WT (Table 1: "Parameters in the model"). The predictions of KO model A at steady-state are summarized in Fig. 2B. Interestingly, although CI activity was reduced by 79% in KO muscle mitochondria the model predicted no change in the maximal PYR oxidation (input of the system) or ATP production (Table 1; "Predicted by the model, Flux values"). The latter was confirmed by experimental analysis (Table 1; "Experimental data, Flux values"). The lack of effect of *NDUFS4*$^{-/-}$ knockout on PYR and ATP fluxes might relate to the fact that mitochondria were isolated from 5-week-old KO mice. At this age the pathophysiological phenotype of the *NDUFS4* gene deletion is still relatively mild [24].

Maximal CS activity was 1.72 higher in KO than in WT mitochondria. This might reflect a general increase in TCA-cycle enzyme level/activity and/or an increase in mitochondrial volume (*e.g.*, [45]). To explore the potential effect of such changes on PYR and ATP fluxes in KO mitochondria we generated two additional KO models (KO model B and C). KO model B was derived from KO model A by increasing the activity of all TCA cycle enzymes by a "CS factor" of 1.72. KO model C was derived from KO model A by increasing the V_{max} of all other enzymes/transporters in the model and mitochondrial volume by the CS-factor of 1.72. KO model B correctly predicted the lack of change in PYR and ATP fluxes, whereas KO model C predicted that these fluxes should be 59–69% higher in KO than in WT mitochondria (Table 1). This suggests that the increase in CS maximal activity might reflect a general increase in the level of TCA enzymes but cannot be considered a measure of mitochondrial volume.

3.5. Metabolic changes in skeletal muscle mitochondria from KO mice

Comparing the predictions of the WT model (Fig. 2A) and those of KO model A (Fig. 2B) highlighted changes in the TCA cycle and metabolite transport system. Interestingly, the TCA cycle was divided into an "upper" and "lower" segment defined by its reaction fluxes (Fig. 2B; lower segment colored green). To the best of our knowledge such a bifurcation of the TCA cycle was not reported previously in CI deficiency. The upper segment consists of reactions of citrate synthase (CS), aconitase (ACO), isocitrate dehydrogenase (ICDH) and malate dehydrogenase (MDH). The lower segment consists of α-ketoglurarate dehydrogenase (α-KGDH), succinyl-CoA synthetase (SCS), succinate dehydrogenase (CII) and fumarase (FUM). In the upper TCA segment, WT steady-state reaction fluxes were more than 3-fold higher than those within the lower segment (Fig. 2A). In the WT case, the flux through ICDH flux (0.89 mM/s) gets divided at the end of the upper half segment of the TCA cycle: 69% of the flux (0.61 mM/s) goes out of the mitochondrial matrix to the IMS *via* the α-ketoglurarate (α-KG)/malate (MAL) antiporter (AKM) mechanism. The latter reaction is also the most active among the three antiporter mechanisms that bring MAL into the mitochondrial matrix to participate in the initial part of the upper segment of the TCA cycle. Utilizing this flux, the upper TCA segment, along with pyruvate dehydrogenase (PDH) generates 3 NADH molecules to fuel CI (Fig. 2A). The remaining part (31%) of the ICDH flux goes to α-KGDH (0.27 mM/s) to enter the lower half of the TCA cycle to fuel CII and also produce 1 ATP and 1 NADH molecule. The two remaining antiport mechanisms for MAL entry into the TCA cycle are the citrate (CIT)/malate (MAL) antiporter (CM) and the succinate (SUC)/malate (MAL) antiporter (SM). Together, CM and SM only contribute 0.5% to the total MAL entry to the matrix (Fig. 2A). Fig. 2A further shows that in WT mitochondria the upper and lower TCA segments mainly provide substrates to CI and CII, respectively. Obviously, the combined action of CI and CII then provides electrons to the other ETC. complexes to sustain the PMF and fuel ATP generation by CV. Of note, a substantial part of the entering PYR does not contribute to ATP production. Every PYR produces 4 NADH after entering the TCA cycle. ATP produced per NADH oxidized, which is same as ATP produced per O_2 consumed, can be calculated simply by dividing the CV flux by the CIV flux. For the WT mice CV/CIV = 7.09/3.20 = 2.22. According to this calculation we should have obtained 363 * 4 * 2.22 = 3223 nmol/h/mg protein ATP, which is 45% higher than the observed ATP flux (Table 1). In the KO mice, the expected ATP production rate is 391 * 4 * (7.03 / 3.19) = 3447 nmol/h/mg protein, which is 65% higher than the experimental value. The lower rate of observed *vs.* predicted ATP production may be due to the absence in the model of other PYR-consuming mechanisms, for instance conversion into lactate (LAC). In addition to the above, analysis of the KO model suggested various changes in other reaction fluxes and metabolite concentrations (Fig. 2B). In the CI-deficient state the lower segment of the TCA cycle carried 10–11% more flux than the WT model. Also the ICDH flux distribution to the lower segment and to the antiport mechanism was altered in the KO model. Of the ICDH flux, 35% is diverted towards the lower segment (31% in WT) and 65% towards the AKM system (69% in WT) to transport MAL into the matrix. Reducing CI activity by 80% only marginally affected its flux. It was also predicted that the flux through the upper part of the TCA cycle was only slightly reduced in KO mitochondria. This reduction is compensated by an increase (11%) in flux through the lower part of the TCA cycle, explaining the absence of effect on the total mitochondrial ATP production rate. The KO model further predicted a change in the steady-state matrix concentration of intermediate metabolites (Fig. 2B). Our predictions are compatible with the results of Mazat et al. [46], where a reduction in ETC. complex activity only slightly affected the fluxes of these complexes but major changes occurred in the concentration of metabolites associated with the affected complexes. With respect to CI, the KO model predicts a reduction in its upstream metabolite (reduced ubiquinol;"QH_2" or ubiquinol: decreased by 65%) and an increased in its downstream metabolite (oxidized ubiquinol; "COQ"or ubiquinone: increased by 11%). Compatible with the measured increase in V_{max} of CII and CIII in KO mitochondria, the KO model predicts a decrease in the concentration of intermediate metabolites downstream of these complexes (*i.e.*, succinate and reduced cytochrome-*c* were down by 71% and 26%, respectively). Similarly, the increased V_{max} of CIII in the KO model was associated with an increase in its upstream metabolites oxidized ubiquinol ('COQ'; by 11%) and oxidized cytochrome-*c* ("C_{ox}"; by 13%). Mitochondrial NADH/NAD^+ ratio and $\Delta\psi$ were predicted to be (slightly) increased and depolarized, respectively. The latter predictions are compatible with results obtained in patient fibroblasts with inherited CI deficiency and cells treated with the CI inhibitor rotenone [28,47].

3.6. Predicting the consequences of CI deficiency

Patients with isolated CI deficiency display a variably reduced CI activity (V_{max}) in muscle homogenates and primary fibroblasts [38]. During the last years, the consequences of isolated CI deficiency in primary patient fibroblasts have been extensively studied at the cellular level [28,31–34]. Native gel electrophoresis revealed variable amounts of holo-CI in patient cells, where in general three patterns were observed (i) the amount of active holo-CI was reduced (mutations in NDUFS2, NDUFS7 or NDUFS8) (ii) the amount of active holo-CI was reduced and a ~830-kDa CI was present (NDUFV1, NDUFS1) (iii) or only a ~830-kDa CI was present (NDUFS4) [48,49]. Analysis of total cell homogenates by Western blotting revealed that the level of the 39-kDa CI subunit was twofold reduced in patient cohorts as compared to the controls, however cellular expression levels of other OXPHOS complex subunits were not altered significantly [33]. To gain further insight into the metabolic consequences of CI activity reduction at steady-state we performed various simulation runs with the WT model using different V_{max} values for CI (*i.e.*, lowering it from 100% to 1% of its normal maximal activity). A complete overview of the numerical data generated by these simulations (*i.e.*, steady-state reaction fluxes, metabolite concentrations and physiological parameters) is provided in

Supplementary Tables S4 and S5. Of note, the WT model was not compatible with a CI activity of 0%, which resulted in all fluxes being zero. The relationship between residual CI activity and key variables in the model is summarized in Fig. 3. Most of the fluxes of the OXPHOS complexes (Fig. 3A), TCA cycle (Fig. 3B) and trans-MIM exchangers (Fig. 3C) were not altered by moderate CI activity reduction. As discussed above, the CII flux increased with decreasing CI activity (Fig. 3A), compatible with the predicted activation of the lower half of the TCA cycle (Fig. 3B).

In general, reaction fluxes became substantially affected when CI activity was reduced by more than 90%. Compatible with our experimental observations and KO model predictions (Table 1), PYR oxidation and ATP production were only substantially reduced when CI activity was lowered by more than 90% (Fig. 3D). The concentration of ATP, ADP, GTP, GDP, P_i (Fig. 3E), TCA intermediates (Fig. 3F), matrix ions (Fig. 3G) and metabolites involved in redox homeostasis (Fig. 3H) was generally not affected by moderate CI activity reduction. Again, these parameters changed when CI activity was reduced by more than 90%.

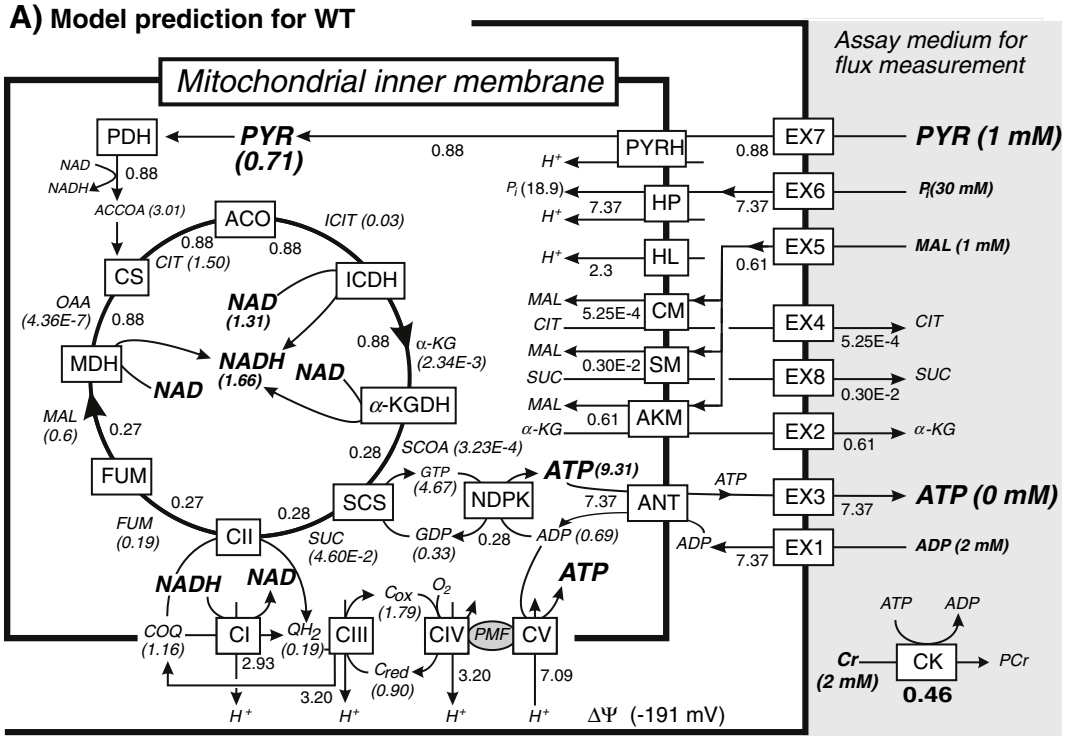

Table 1
Maximal mitochondrial enzyme activities, pyruvate oxidation and ATP production in isolated skeletal muscle mitochondria from WT and KO mice.

V_{max} values	Experimental data			Parameters in the model		
	WT	KO	KO/WT	KO model A	KO model B	KO model C[a]
CI (mU/mg)[d]	34 ± 7.2	7.2 ± 2.0*	0.21	V_{max} × 0.21	V_{max} × 0.21	V_{max} × 0.21
CII (mU/mg)[d]	36 ± 4.9	56 ± 6.3*	1.56	V_{max} × 1.56	V_{max} × 1.56	V_{max} × 1.56
CIII (mU/mg)[d]	278 ± 39.4	404 ± 45.2	1.45	V_{max} × 1.45	V_{max} × 1.45	V_{max} × 1.45
CIV (mU/mg)[d]	257 ± 54.6	437 ± 34.9*	1.7	V_{max} × 1.70	V_{max} × 1.70	V_{max} × 1.70
CS (mU/mg)[d]	227 ± 44.3	390 ± 32.2*	1.72	V_{max} × 1.72	V_{max} × 1.72	V_{max} × 1.72
TCA cycle enzymes[b]	n.d.	n.d.	n.d.	Like in WT model	V_{max} × 1.72	V_{max} × 1.72
Transport reactions[c]	n.d.	n.d.	n.d.	Like in WT model	Like in WT model	V_{max} × 1.72
Flux values	**Experimental data**			**Predicted by the model**		
PYR oxidation (nmol/h/mg)[d]	363 ± 52.7	391 ± 113	1.08	**KO/WT** = 0.97	**KO/WT** = 0.94	**KO/WT** = 1.59
ATP production (nmol/h/mg)[d]	1776 ± 251.7	1532 ± 326.3	0.86	**KO/WT** = 1.00	**KO/WT** = 1.00	**KO/WT** = 1.69

Abbreviations: CI, complex I; CII, complex II or succinate dehydrogenase (SDH); CIII, complex III; CIV, complex IV; CS, citrate synthase; KO, knockout; V_{max}, maximal activity; WT, wild type.
Statistics: Average values were obtained from 5 individual animals.
[a] In model C also the V_{max} of CV and NDPK (Fig. 2) are increased by a factor of 1.72. In the latter model also the V_{max} of GOT (Glutamate oxaloacetate transporter), GLUH (Glutamate/H^+-cotransporter), AG (Aspartate/Glutamate-antitransporter), GLUT (Glutamate exchanger), ASPt (Aspartate exchanger), MALP (Malate/Phosphate antitransporter) and KH (K^+/H^+-antiporter) were increased by a factor of 1.72. However, the reactions involving these enzymes/transporters are not in Fig. 2 because their predicted flux equals zero.
[b] All enzymes participating in the TCA cycle in addition to CII and CS (*i.e.*, PDH, ACO, ICDH, α-KGHD, SCS, FUM and MDH; Fig. 2).
[c] All transport reactions across the mitochondrial inner and outer membrane (*i.e.*, ANT, AKM, CM, HL, HP, PYRH, SM, EX1, EX2, EX3, EX4, EX5, EX6, EX7, EX8; Fig. 2).
[d] Normalized on mg protein.
* ($P < 0.05$) relative to WT.

This suggests that steady-state energy homeostasis under non substrate-limited conditions is not affected as long as a certain (critical) amount of residual CI activity remains. In other words, CI activity can be inhibited to a certain threshold value (in our case near to 90% inhibition) before its metabolic consequences become. Similar observations were made in various rotenone-treated rat tissues, where mitochondrial O_2 consumption substantially dropped only when CI was inhibited by more than 80% [46,52,53]. Overcapacity of OXPHOS complexes is not specific for CI [46,50]. For instance, a reduction in CIV activity by almost 50% was virtually without effect on CIV flux and O_2 consumption in patient cells [46,54].

Metabolic control analysis (MCA) of the WT model revealed that the control coefficient for CI equaled 0.013, which was lower than a previously reported value ([50]). Our model also predicted control coefficients for CII, CIII, CIV and CV (see Supplementary Fig. S1) that were lower than previously reported values [50]. In general, lower control coefficients are associated with a higher threshold value [46,51]. In this sense, the high CI threshold value predicted by our model might be overestimated. This could be due the fact that although the original model was parametrized using experimental data [39], it was not a skeletal muscle-specific model. Compatible with previous results in genetic and inhibitor-induced fibroblast models of CI deficiency [25,28,38], the WT model predicted that a reduction in CI activity was associated with redox alterations (*e.g.*, an increase in NADH/NAD^+ ratio; Fig. 3H) and partial $\Delta\psi$ depolarization (Fig. 3I).

4. Summary and conclusion

This study combines experimental and *in silico* strategies to gain insight into the consequences of isolated mitochondrial CI deficiency in isolated skeletal muscle mitochondria from *NDUFS4*$^{-/-}$ mice. We demonstrate that *NDUFS4*$^{-/-}$ gene deletion reduces maximal CI activity and is paralleled by increased activity of CII, CIII, CIV and CS. Surprisingly, *NDUFS4* knockout did not affect the maximal rate of PYR oxidation and ATP production. Mathematical modeling suggests that this phenomenon might be due to increased activity of the lower half of the TCA cycle, including CII. It further appears that mouse skeletal muscle mitochondria possess a substantial CI overcapacity, which further minimizes the effects of partial CI deficiency on mitochondrial metabolism. This means that CI activity can be inhibited to a certain threshold value (in our case near to 90% inhibition) before its metabolic consequences become apparent. We conclude that these consequences in CI-deficient KO mitochondria are minimized by CII-mediated fueling of the OXPHOS system and CI overcapacity. This still leaves open the possibility that mitochondrial ATP generation becomes limited when energy substrates are scarce and/or cellular energy demands increase during cell activation.

Transparency document

The Transparency document associated with this article can be found, in the online version.

Acknowledgments

This work was supported by the CSBR (Centre for Systems Biology Research) initiative from the Netherlands Organisation for Scientific Research (NWO; No: CSBR09/013V). We are grateful to Dr. D.A. Beard (Department of Molecular and Integrative Physiology, University of

Fig. 2. Predicted metabolic consequences of mitochondrial complex I deficiency in isolated mouse skeletal muscle mitochondria. (A) Isolated mitochondria were placed in an assay medium (gray) for experimental analysis. This was modeled using the depicted metabolic network containing exchange fluxes, TCA cycle and the mitochondrial oxidative phosphorylation (OXPHOS) system. Numerals represent the predicted steady-state values of fluxes (in mmol s^{-1} (l mito volume)$^{-1}$ or mmol s^{-1} (l cyto volume)$^{-1}$) and metabolite concentrations (in mM) for the WT situation. (B) Similar to panel A, but now for mitochondria from *NDUFS4*$^{-/-}$ (KO) animals. Colors indicate whether a flux or concentration is increased (green), decreased (red) or not affected (white) in the KO model. Abbreviations: ACCOA, acetyl-CoA; ACO, aconitase; ADP, adenosine diphosphate; AKM, α-ketoglurarate (α-KG)/malate (MAL) antiporter; ANT, adenine nucleotide translocase; ATP, adenosine triphosphate; CI, complex I; CII, complex II or succinate dehydrogenase; CIII, complex III; CIT, citrate; CIV, complex IV; CK, creatine kinase; CM, citrate (CIT)/malate (MAL) antiporter; COQ, oxidized ubiquinol; Cox, oxidized cytochrome-c; Cred, reduced cytochrome-c; CS, citrate synthase; CV, complex V or FoF1-ATPase; EX1, ADP exchange with assay medium; EX2, α-KG exchange with assay medium; EX3, ATP exchange with assay medium; EX4, CIT exchange with assay medium; EX5, MAL exchange with assay medium; EX6, Pi exchange with assay medium; EX7, PYR exchange with assay medium; EX8, SUC exchange with assay medium; FUM, Fumarase; FUM, fumarate; GDP, guanosine diphosphate; GTP, guanosine triphosphate; H^+, hydrogen; HL, H^+-leak; HP, H^+-Pi cotransporter; ICDH, isocitrate dehydrogenase; ICIT, isocitrate; MAL, malate; MDH, malate dehydrogenase; NAD^+, nicotinamide adenine dinucleotide; NADH, reduced NAD^+; NDPK, nucleoside diphosphokinase; OAA, oxaloacetate; PDH, pyruvate dehydrogenase; Pi, inorganic phosphate; PYR, pyruvate; PYRH, PYR-H^+ cotransporter; QH_2, reduced ubiquinol; SCOA, succinyl-CoA; SCS, succinyl-CoA synthetase; SM, succinate (SUC)/malate (MAL) antiporter; SUC, succinate; α-KG, α-ketoglutarate; α-KGDH, α-ketoglurarate dehydrogenase; $\Delta\psi$, mitochondrial membrane potential.

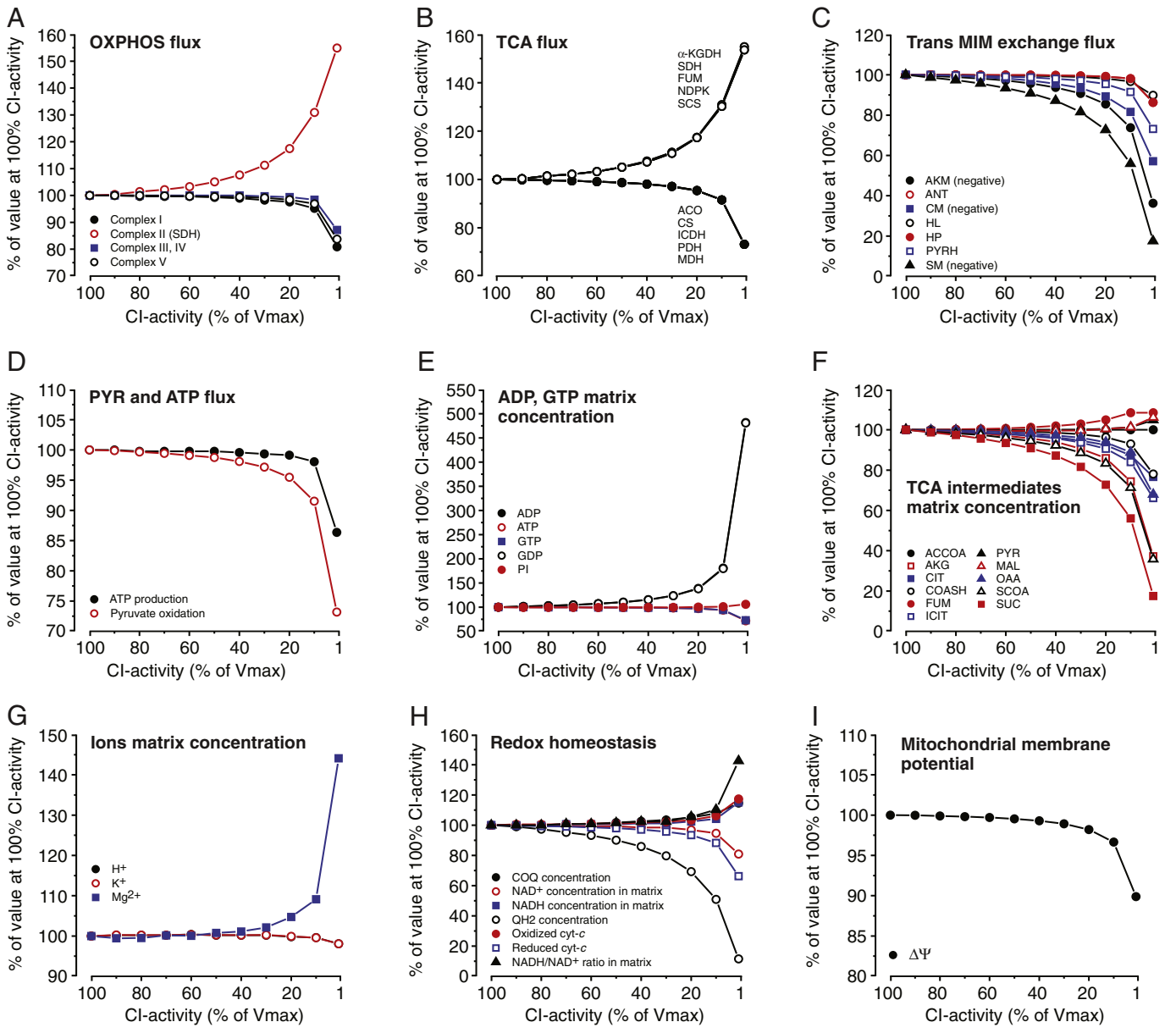

Fig. 3. Predicted consequences of CI deficiency in isolated mouse skeletal muscle mitochondria. The V_{max} of CI (x-axis) was gradually reduced from 100% to 1% of that in the WT model and the effect on various steady-state metabolic fluxes, concentrations and other variables was predicted. To facilitate visual inspection, values on the y-axis were expressed as % of their value at 100% CI activity. (A) Effect of increasing CI deficiency on the flux through the OXPHOS system (CI, CII, CIII = CIV, and CV). (B) Similar to panel A, but now for TCA fluxes. (C) Similar to panel A, but now for exchange fluxes across the mitochondrial inner membrane (MIM). (D) Similar to panel A, but now for pyruvate (PYR) and ATP fluxes. (E) Similar to panel A, but now for ADP and GTP concentration in the mitochondrial matrix. (F) Similar to panel A, but now for TCA cycle intermediates. (G) Similar to panel A, but now for the free concentration of H^+, K^+ and Mg^{2+} in the mitochondrial matrix. (H) Similar to panel A, but now for redox-related parameters. (I) Similar to panel A, but now for mitochondrial membrane potential $\Delta\psi$ (See main text for details).

Michigan, Ann Arbor, Michigan, USA) for supplying us with the original model.

Appendix A. Supplementary data

Supplementary data to this article can be found online at http://dx.doi.org/10.1016/j.bbabio.2015.02.006.

References

[1] D.D. Newmeyer, S. Ferguson-Miller, Mitochondria: releasing power for life and unleashing the machineries of death, Cell 112 (2003) 481–490.
[2] M.R. Duchen, Mitochondria in health and disease: perspectives on a new mitochondrial biology, Mol. Asp. Med. 25 (2004) 365–451. http://dx.doi.org/10.1016/j.mam.2004.03.001.
[3] R.S. Balaban, S. Nemoto, T. Finkel, Mitochondria, oxidants, and aging, Cell 120 (2005) 483–495. http://dx.doi.org/10.1016/j.cell.2005.02.001.
[4] S.A. Detmer, D.C. Chan, Functions and dysfunctions of mitochondrial dynamics, Nat. Rev. Mol. Cell Biol. 8 (2007) 870–879. http://dx.doi.org/10.1038/nrm2275.
[5] A. Tzagoloff, Mitochondria, Plenum Press, 1982.
[6] H.M. McBride, M. Neuspiel, S. Wasiak, Mitochondria: more than just a powerhouse, Curr. Biol. 16 (2006) R551–R560. http://dx.doi.org/10.1016/j.cub.2006.06.054.
[7] P. Siekevitz, Powerhouse of the Cell, Freeman, 1957.
[8] G. Kroemer, Mitochondrial control of apoptosis: an overview, Biochem. Soc. Symp. 66 (1999) 1–15.
[9] C.E.J. Dieteren, S.C.A.M. Gielen, L.G.J. Nijtmans, J.A.M. Smeitink, H.G. Swarts, R. Brock, et al., Solute diffusion is hindered in the mitochondrial matrix, Proc. Natl. Acad. Sci. 108 (2011) 8657–8662. http://dx.doi.org/10.1073/pnas.1017581108.
[10] S. Herzig, E. Raemy, S. Montessuit, J.-L. Veuthey, N. Zamboni, B. Westermann, et al., Identification and functional expression of the mitochondrial pyruvate carrier, Science 337 (2012) 93–96. http://dx.doi.org/10.1126/science.1218530.
[11] W.J.H. Koopman, P.H.G.M. Willems, J.A.M. Smeitink, Monogenic mitochondrial disorders, N. Engl. J. Med. 366 (2012) 1132–1141. http://dx.doi.org/10.1056/NEJMra1012478.

[12] A.H.V. Schapira, Mitochondrial disease, Lancet 368 (2006) 70–82. http://dx.doi.org/10.1016/S0140-6736(06)68970-8.

[13] S. DiMauro, E.A. Schon, Mitochondrial respiratory-chain diseases, N. Engl. J. Med. 348 (2003) 2656–2668. http://dx.doi.org/10.1056/NEJMra022567.

[14] P.E. Coskun, M.F. Beal, D.C. Wallace, Alzheimer's brains harbor somatic mtDNA control-region mutations that suppress mitochondrial transcription and replication, Proc. Natl. Acad. Sci. U. S. A. 101 (2004) 10726–10731. http://dx.doi.org/10.1073/pnas.0403649101.

[15] S.H. Kim, R. Vlkolinsky, N. Cairns, M. Fountoulakis, G. Lubec, The reduction of NADH: ubiquinone oxidoreductase 24- and 75-kDa subunits in brains of patients with Down syndrome and Alzheimer's disease, Life Sci. 68 (2001) 2741–2750. http://dx.doi.org/10.1016/S0024-3205(01)01074-8.

[16] J. Finsterer, Central nervous system manifestations of mitochondrial disorders, Acta Neurol. Scand. 114 (2006) 217–238. http://dx.doi.org/10.1111/j.1600-0404.2006.00671.x.

[17] M. Orth, A.H. Schapira, Mitochondrial involvement in Parkinson's disease, Neurochem. Int. 40 (2002) 533–541. http://dx.doi.org/10.1016/S0197-0186(01)00124-3.

[18] D.M. Kirby, M. Crawford, M.A. Cleary, H.H. Dahl, X. Dennett, D.R. Thorburn, Respiratory chain complex I deficiency: an underdiagnosed energy generation disorder, Neurology 52 (1999) 1255–1264.

[19] J.L. Loeffen, J.A. Smeitink, J.M. Trijbels, A.J. Janssen, R.H. Triepels, R.C. Sengers, et al., Isolated complex I deficiency in children: clinical, biochemical and genetic aspects, Hum. Mutat. 15 (2000) 123–134. http://dx.doi.org/10.1002/(SICI)1098-1004(200002)15:2<123::AID-HUMU1>3.0.CO;2-P.

[20] J. Smeitink, R. Sengers, F. Trijbels, L. van den Heuvel, Human NADH:ubiquinone oxidoreductase, J. Bioenerg. Biomembr. 33 (2001) 259–266. http://dx.doi.org/10.1023/A:1010743321800.

[21] J. Smeitink, L. van den Heuvel, S. DiMauro, The genetics and pathology of oxidative phosphorylation, Nat. Rev. Genet. 2 (2001) 342–352. http://dx.doi.org/10.1038/35072063.

[22] P. Benit, J. Steffann, S. Lebon, D. Chretien, N. Kadhom, P. de Lonlay, et al., Genotyping microsatellite DNA markers at putative disease loci in inbred/multiplex families with respiratory chain complex I deficiency allows rapid identification of a novel nonsense mutation (IVS1nt −1) in the NDUFS4 gene in Leigh syndrome, Hum. Genet. 112 (2003) 563–566. http://dx.doi.org/10.1007/s00439-002-0884-2.

[23] J. Carroll, I.M. Fearnley, J.M. Skehel, R.J. Shannon, J. Hirst, J.E. Walker, Bovine complex I is a complex of 45 different subunits, J. Biol. Chem. 281 (2006) 32724–32727. http://dx.doi.org/10.1074/jbc.M607135200.

[24] S.E. Kruse, W.C. Watt, D.J. Marcinek, R.P. Kapur, K.A. Schenkman, R.D. Palmiter, Mice with mitochondrial complex I deficiency develop a fatal encephalomyopathy, Cell Metab. 7 (2008) 312–320. http://dx.doi.org/10.1016/j.cmet.2008.02.004.

[25] F. Distelmaier, W.J.H. Koopman, L.P. van den Heuvel, R.J. Rodenburg, E. Mayatepek, P.H.G.M. Willems, et al., Mitochondrial complex I deficiency: from organelle dysfunction to clinical disease, Brain 132 (2009) 833–842. http://dx.doi.org/10.1093/brain/awp058.

[26] E. Fassone, S. Rahman, Complex I deficiency: clinical features, biochemistry and molecular genetics, J. Med. Genet. 49 (2012) 578–590. http://dx.doi.org/10.1136/jmedgenet-2012-101159.

[27] W.J.H. Koopman, F. Distelmaier, J.A. Smeitink, P.H. Willems, OXPHOS mutations and neurodegeneration, EMBO J. 32 (2013) 9–29. http://dx.doi.org/10.1038/emboj.2012.300.

[28] W.J.H. Koopman, L.G.J. Nijtmans, C.E.J. Dieteren, P. Roestenberg, F. Valsecchi, J.A.M. Smeitink, et al., Mammalian mitochondrial complex I: biogenesis, regulation, and reactive oxygen species generation, Antioxid. Redox Signal. 12 (2010) 1431–1470. http://dx.doi.org/10.1089/ars.2009.2743.

[29] E. Balsa, R. Marco, E. Perales-Clemente, R. Szklarczyk, E. Calvo, M.O. Landázuri, et al., NDUFA4 is a subunit of complex IV of the mammalian electron transport chain, Cell Metab. 16 (2012) 378–386. http://dx.doi.org/10.1016/j.cmet.2012.07.015.

[30] J. Nouws, L.G.J. Nijtmans, J.A. Smeitink, R.O. Vogel, Assembly factors as a new class of disease genes for mitochondrial complex I deficiency: cause, pathology and treatment options, Brain J. Neurol. 135 (2012) 12–22. http://dx.doi.org/10.1093/brain/awr261.

[31] H.-J. Visch, G.A. Rutter, W.J.H. Koopman, J.B. Koenderink, S. Verkaart, T. de Groot, et al., Inhibition of mitochondrial Na^+–Ca^{2+} exchange restores agonist-induced ATP production and $Ca2^+$ handling in human complex I deficiency, J. Biol. Chem. 279 (2004) 40328–40336. http://dx.doi.org/10.1074/jbc.M408068200.

[32] W.J.H. Koopman, H.-J. Visch, S. Verkaart, L.W.P.J. van den Heuvel, J.A.M. Smeitink, P.H.G.M. Willems, Mitochondrial network complexity and pathological decrease in complex I activity are tightly correlated in isolated human complex I deficiency, Am. J. Physiol. Cell Physiol. 289 (2005) C881–C890. http://dx.doi.org/10.1152/ajpcell.00104.2005.

[33] W.J.H. Koopman, S. Verkaart, H.J. Visch, S. van Emst-de Vries, L.G.J. Nijtmans, J.A.M. Smeitink, et al., Human NADH:ubiquinone oxidoreductase deficiency: radical changes in mitochondrial morphology? Am. J. Physiol. Cell Physiol. 293 (2007) C22–C29. http://dx.doi.org/10.1152/ajpcell.00194.2006.

[34] W.J.H. Koopman, S. Verkaart, S.E. van Emst-de Vries, S. Grefte, J.A.M. Smeitink, L.G.J. Nijtmans, et al., Mitigation of NADH: ubiquinone oxidoreductase deficiency by chronic Trolox treatment, Biochim. Biophys. Acta 1777 (2008) 853–859. http://dx.doi.org/10.1016/j.bbabio.2008.03.028.

[35] P.H.G.M. Willems, F. Valsecchi, F. Distelmaier, S. Verkaart, H.-J. Visch, J.A.M. Smeitink, et al., Mitochondrial $Ca2^+$ homeostasis in human NADH:ubiquinone oxidoreductase deficiency, Cell Calcium 44 (2008) 123–133. http://dx.doi.org/10.1016/j.ceca.2008.01.002.

[36] P.H.G.M. Willems, J.A.M. Smeitink, W.J.H. Koopman, Mitochondrial dynamics in human NADH:ubiquinone oxidoreductase deficiency, Int. J. Biochem. Cell Biol. 41 (2009) 1773–1782. http://dx.doi.org/10.1016/j.biocel.2009.01.012.

[37] L. van den Heuvel, W. Ruitenbeek, R. Smeets, Z. Gelman-Kohan, O. Elpeleg, J. Loeffen, et al., Demonstration of a new pathogenic mutation in human complex I deficiency: a 5-bp duplication in the nuclear gene encoding the 18-kD (AQDQ) subunit, Am. J. Hum. Genet. 62 (1998) 262–268. http://dx.doi.org/10.1086/301716.

[38] F. Valsecchi, C. Monge, M. Forkink, A.J.C. de Groof, G. Benard, R. Rossignol, et al., Metabolic consequences of NDUFS4 gene deletion in immortalized mouse embryonic fibroblasts, Biochim. Biophys. Acta 1817 (2012) 1925–1936. http://dx.doi.org/10.1016/j.bbabio.2012.03.006.

[39] F. Wu, F. Yang, K.C. Vinnakota, D.A. Beard, Computer modeling of mitochondrial tricarboxylic acid cycle, oxidative phosphorylation, metabolite transport, and electrophysiology, J. Biol. Chem. 282 (2007) 24525–24537. http://dx.doi.org/10.1074/jbc.M701024200.

[40] A.J.M. Janssen, F.J.M. Trijbels, R.C.A. Sengers, L.T.M. Wintjes, W. Ruitenbeek, J.A.M. Smeitink, et al., Measurement of the energy-generating capacity of human muscle mitochondria: diagnostic procedure and application to human pathology, Clin. Chem. 52 (2006) 860–871. http://dx.doi.org/10.1373/clinchem.2005.062414.

[41] R.J.T. Rodenburg, Biochemical diagnosis of mitochondrial disorders, J. Inherit. Metab. Dis. 34 (2011) 283–292. http://dx.doi.org/10.1007/s10545-010-9081-y.

[42] M.C. Kohn, M.J. Achs, D. Garfinkel, Computer simulation of metabolism in pyruvate-perfused rat heart. III. Pyruvate dehydrogenase, Am. J. Physiol. 237 (1979) R167–R173.

[43] M.C. Kohn, D. Garfinkel, Computer simulation of metabolism in palmitate-perfused rat heart. II. Behavior of complete model, Ann. Biomed. Eng. 11 (1983) 511–531. http://dx.doi.org/10.1007/BF02364082.

[44] S. Bose, S. French, F.J. Evans, F. Joubert, R.S. Balaban, Metabolic network control of oxidative phosphorylation: multiple roles of inorganic phosphate, J. Biol. Chem. 278 (2003) 39155–39165. http://dx.doi.org/10.1074/jbc.M306409200.

[45] K.J. Tronstad, M. Nooteboom, L.I.H. Nilsson, J. Nikolaisen, M. Sokolewicz, S. Grefte, et al., Regulation and quantification of cellular mitochondrial morphology and content, Curr. Pharm. Des. 20 (2014) 5634–5652.

[46] J.P. Mazat, R. Rossignol, M. Malgat, C. Rocher, B. Faustin, T. Letellier, What do mitochondrial diseases teach us about normal mitochondrial functions…that we already knew: threshold expression of mitochondrial defects, Biochim. Biophys. Acta 1504 (2001) 20–30.

[47] F. Distelmaier, W.J.H. Koopman, L.P. van den Heuvel, R.J. Rodenburg, E. Mayatepek, P.H.G.M. Willems, et al., Mitochondrial complex I deficiency: from organelle dysfunction to clinical disease, Brain J. Neurol. 132 (2009) 833–842. http://dx.doi.org/10.1093/brain/awp058.

[48] F. Valsecchi, W.J.H. Koopman, G.R. Manjeri, R.J. Rodenburg, J.A.M. Smeitink, P.H.G.M. Willems, Complex I disorders: causes, mechanisms, and development of treatment strategies at the cellular level, Dev. Disabil. Res. Rev. 16 (2010) 175–182. http://dx.doi.org/10.1002/ddrr.107.

[49] L. Blanchet, L.M.C. Buydens, J.A.M. Smeitink, P.H.G.M. Willems, W.J.H. Koopman, Isolated mitochondrial complex I deficiency: explorative data analysis of patient cell parameters, Curr. Pharm. Des. 17 (2011) 4023–4033. http://dx.doi.org/10.2174/138161211798764870.

[50] G.P. Davey, J.B. Clark, Threshold effects and control of oxidative phosphorylation in nonsynaptic rat brain mitochondria, J. Neurochem. 66 (1996) 1617–1624.

[51] R. Rossignol, T. Letellier, M. Malgat, C. Rocher, J.P. Mazat, Tissue variation in the control of oxidative phosphorylation: implication for mitochondrial diseases, Biochem. J. 347 (Pt 1) (2000) 45–53.

[52] R. Rossignol, M. Malgat, J.-P. Mazat, T. Letellier, Threshold effect and tissue specificity: implication for mitochondrial cytopathies, J. Biol. Chem. 274 (1999) 33426–33432.

[53] M. Malgat, T. Letellier, S.L. Jouaville, J.-P. Mazat, Value of control theory in the study of cellular metabolism — biomedical implications, J. Biol. Syst. 03 (1995) 165–175. http://dx.doi.org/10.1142/S0218339095000162.

[54] A.V. Kuznetsov, J.F. Clark, K. Winkler, W.S. Kunz, Increase of flux control of cytochrome c oxidase in copper-deficient mottled brindled mice, J. Biol. Chem. 271 (1996) 283–288. http://dx.doi.org/10.1074/jbc.271.1.283.